Category-level Part-based 3D Object Non-rigid Registration

Diego Rodriguez[a], Florian Huber and Sven Behnke[b]

Autonomous Intelligent Systems, University of Bonn, Bonn, Germany
{f_author, s_author}@ais.uni-bonn.de

Keywords: Non-rigid Registration, Robot Vision, Shape Spaces.

Abstract: In this paper, we propose a novel approach for registering objects in a non-rigid manner based on decomposed parts of an object category. By performing part-based registration, the deforming points match better local geometric structures of the observed instance. Moreover, the knowledge acquired of an object part can be transferred to different object categories that share the same decomposed part. This is possible because the registration is based on a learned latent space that encodes typical geometrical variations of each part independently. We evaluate our approach extensively on different object categories and demonstrate its robustness against outliers, noise and misalignments of the object pose.

1 INTRODUCTION

The non-rigid registration problem aims to model the deformation between two different feature sets such as meshes or point clouds. The underlying transformation between the sets is unknown, which makes the non-rigid registration problem challenging. These kind of registrations are used in several applications such as medical imaging, object reconstruction and robot vision tasks (Krebs et al., 2017; Zollhöfer et al., 2014; Stouraitis et al., 2015). Particularly, non-rigid registration methods are employed in robot grasping applications in order to transfer knowledge between object instances (Stouraitis et al., 2015; Stueckler et al., 2011; Rodriguez et al., 2018). In this manner, associated grasping knowledge of an object instance is adapted to a novel one based on its geometry. The approach presented in this paper is intended to be used for grasping transfer knowledge.

Online robot grasping tasks pose several challenges in terms of perception and planning. One of these difficulties lies in the inference of the non-observable (from the robot camera perspective) portions of the novel instance, especially because multiple plausible geometries can explain the current observed geometry. Data-driven approaches, as the one presented in this paper, often learn latent spaces of the object category for generating plausible shapes based on the data presented during training (Allen et al., 2003; Burghard et al., 2013; Rodriguez and Behnke,

---
[a] https://orcid.org/0000-0002-1416-7392
[b] https://orcid.org/0000-0002-5040-7525

2018). Thanks to the embedded knowledge in these latent spaces, the reconstruction can be performed online.

In this paper, we propose a novel approach for registering instances belonging to the same object category that registers decomposed parts independently. Our approach is inspired by the observation that some object parts are common across different categories. For example, a chair and a table both contain legs with similar geometries and handles often have similar shape and function. In this manner, knowledge acquired from an object category can be transferred to another. In addition, the registration by parts can increase the registration accuracy of local structures by reducing the number of constraints and degrees of freedom a holistic registration of complex geometries requires.

The main contribution of this paper is the formulation of a novel approach for part-based non-rigid registration that can be employed for transferring grasping knowledge for online robot applications. We evaluate our approach on different categories and demonstrate that our part-based algorithms achieve better results compared to a holistic-only registration. In addition, we create a new dataset that contains meshes and corresponding point clouds together with the respective part decomposition. The part segmentation is done manually to express semantic concepts and to ensure the quality of the dataset. The dataset and the source code of our implementation will be released upon acceptance.

Our approach is especially robust against occlusions because of the embedded knowledge in the learned shape spaces. Thus, this it is very relevant for online robot applications where objects are not fully observable.

2 RELATED WORK

Different approaches have been proposed to address the non-rigid registration problem according to the restrictions of the deforming point set to match the observed one. The most widely used constraints include: conformal maps (Kim et al., 2011; Zeng et al., 2010), isometry (Tevs et al., 2009; Ovsjanikov et al., 2010), thin-plate splines (Chui and Rangarajan, 2003; Zou et al., 2007), Gaussian fields (Haehnel et al., 2003), and motion coherence theory (Myronenko and Song, 2010). The non-rigid registration has been also formulated as a probability density estimation problem (Myronenko and Song, 2010; Horaud et al., 2010; Ma et al., 2016), where parameters of Gaussian Mixture Models (GMMs) are optimized by means of the Expectation Maximization (EM) algorithm. The Coherent Point Drift (CPD) algorithm (Myronenko and Song, 2010) makes use of such methods.

These traditional algorithms, however, have difficulties with partially observed data, because they do not incorporate any information on the observed point sets. Shape priors and latent spaces are frequently used to address this issue with different feature sets such as body shapes (Allen et al., 2003; Hasler et al., 2009), brain images (Marsland et al., 2003), faces (Blanz and Vetter, 1999), and collections of shapes (Nguyen et al., 2011; Huang et al., 2012). Dense correspondences can be also inferred based on a compact shape space of similar shapes (Burghard et al., 2013; Engelmann et al., 2016).

The decomposition of complex object geometries into parts holds the promise to reduce the registration error. In (Adeshina and Cootes, 2010), an image-based approach was developed to find correspondences between segment parts of bones and their location. Dense correspondences between 3D shapes have been also estimated by considering independent parts (Burghard et al., 2013). A hierarchical approach for registering 2D point sets was proposed in (Xiong et al., 2018). The method iteratively segments a 2D point cloud in different parts and finds the deformations of each individual part in an ICP (Iterative Closest Point) manner. Similarly, several grasping planning approaches aim to reduce complexity by transferring grasp skills between simpler parts or geometrical primitives (cylinders, boxes, spheres) (Aleotti and

Caselli, 2011; Aleotti et al., 2014; Vahrenkamp et al., 2016).

3 PART-BASED NON-RIGID REGISTRATION

We propose a learning-based approach for registering instances belonging to an object category in a non-rigid manner which considers both the complete geometry of the objects and their decomposed parts. We define a category as a set objects with similar extrinsic geometry and usage, e.g., *drill*, *spray bottle*, etc. Our method defines a training phase in which multiple shape spaces are learned based on the point sets of the training instances. A shape space is a low-dimensional manifold that describes typical intra-class geometrical variations. The construction of these spaces is explained in Section 3.1. The learned shape spaces are used during inference for finding geometries that match best the observed ones. This search is formulated as an optimization problem as described in Section 3.2. For a category with p number of parts, $p+1$ shape spaces are learned: one for each part and an additional one for the entire not decomposed instances. This additional shape space is referred as the holistic shape space. Our approach has two variants: *partwise* and *hol+part*. The former formulates the non-rigid registration as the result of independent parallel registrations for each object part (Figure 1). The latter performs first a holistic registration to capture the global features and to initialize the search inside the shape spaces of the decomposed parts. Comparisons between both variants are presented in the evaluation (Section 4).

3.1 Shape Space

The shape spaces presented here are constructed based on a collection of training 3D point sets. From the collection, a 3D point set is selected as the canonical model $\mathbf{C} \in \mathbb{R}^{M \times 3} = (\mathbf{c}_1, \cdots, \mathbf{c}_M)^T$ which represents a nominal instance of the collection, where M represents the number of 3D points in $\mathbf{C}$. The canonical model is then registered non-rigidly towards each of the remaining training point sets $\mathbf{T_i}$ by means of the Coherent Point Drift (CPD) algorithm (Myronenko and Song, 2010). Note that all object frames are aligned before performing the registration. In the mug category, for example, all axes of the cylinders are aligned and all handles are placed in the same position. The resulting registered point set $\mathcal{T}_i$ is formulated as:

$$\mathcal{T}_i(\mathbf{C}, \mathbf{W}_i) = \mathbf{C} + \mathbf{G}\mathbf{W}_i, \tag{1}$$
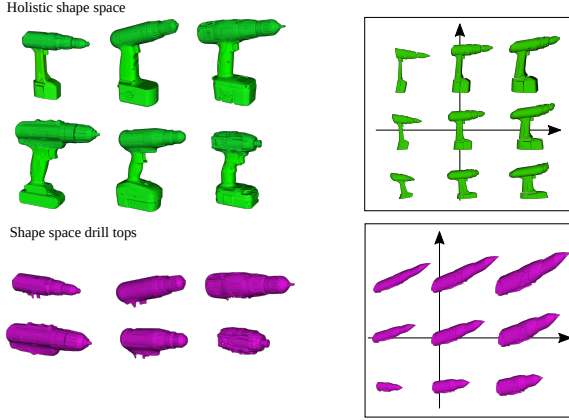
Figure 1: Category-level part-based registration. Multiple shape (latent) spaces are learned. Initially, a *holistic* shape space of the entire geometries is learned. Then, for each of the parts, an individual shape space is constructed following the same algorithm, i.e., by computing deformation fields using CPD and by finding a lower-dimensional space using PCA-EM. For example, the drill category will establish four shape spaces, one holistic (green), and one for each of the parts: shank, base and top (magenta).

where $\mathbf{G}$ is a Gaussian kernel matrix defined element-wise as:

$$g_{ij} := G(\mathbf{c}_i, \mathbf{c}_j) = \exp^{-\frac{1}{2\beta^2}\|\mathbf{c}_i - \mathbf{c}_j\|^2}, \qquad (2)$$

and $\mathbf{W}_i \in \mathbb{R}^{M \times 3}$ is a matrix of kernel weights which can be interpreted as unnormalized deformation field matrix. The deduction of these matrices is out of the scope of this paper, please refer to (Myronenko and Song, 2010) for an in-depth analysis.

Interestingly, the registration is uniquely captured by the matrix $\mathbf{W}_i$ since $\mathbf{C}$ is the same across all training instances, i.e., $\mathbf{G}$ depends only on the canonical model $\mathbf{C}$. Moreover, the dimensionality of $\mathbf{W}_i$ also remains constant for all registrations and more importantly it is ordered, such that a k-row corresponds to a 3D deformation vector of the k-point in $\mathbf{C}$. This allows us to find a lower-dimensional latent space by finding the principal components of all these deformation field matrices $\mathbf{W}_i$. This latent space is calculated by the Principal Component Analysis - Expectation Maximization (PCA-EM) algorithm.

The top of Figure 1 shows a holistic learned shape space of a drill category. Note that the presented principal components correlate qualitatively with the width and the height of the instances.

3.2 Part-based Registration

The input of our approach is a point set belonging to an object category, for instance, a point cloud com-

ing from real sensory data (e.g., a RGB-D camera). As result of the registration, the canonical point set is deformed to match the geometry of a novel observed instance. In this manner, the observed object is reconstructed. In addition, a deformation field is inferred which can be used to transform points and 3D frames associated to the canonical model.

Novel category-like shapes can be generated by interpolating and extrapolating in the shape spaces. In this manner, the non-rigid registration of shapes, either of the entire object or of an object part, is formulated as an optimization problem that minimizes the closest distance between the observed point set $\mathbf{O}$ and the deformed one $\mathcal{T}(\mathbf{C}, \mathbf{W}m(\mathbf{x}))$. The energy function to minimize is formulated as:

$$E(\mathbf{x}, \boldsymbol{\theta}) = \sum_{m=1}^{M} \min_{n} \|\mathbf{O}_n - \Theta(\mathcal{T}(\mathbf{C}_m, \mathbf{W}_m(\mathbf{x})), \boldsymbol{\theta})\|^2.$$
$$(3)$$

where $\boldsymbol{\theta}$ defines the parameters of a rigid transformation incorporated to account for misalignments of the observed object pose and Θ is a function that applies this rigid transformation. A good initialization of the object pose is however required because of many local minima of the optimization problem. In Equation (3), the notation $\mathbf{A}_n$ refers to the point n of matrix $\mathbf{A}$. Note that by the incorporation of the rigid term, the optimization becomes non-linear. This optimization problem is solved by using the *ceres* optimizer[1].

In order to improve the registration accuracy of complex local structures, our approach includes the registration of each object part independently. Therefore, initially, the objects are decomposed into simpler parts. The decomposition is done manually by experts to express semantic concepts and to ensure the quality of the segmentation. Automatic approaches such as (Araslanov et al., 2016; Palafox et al., 2021) are alternatives to perform the part decomposition.

The *partwise* variant registers each part independently. In this manner, for an object with three parts, three different shape spaces will be learned and three different optimization problems will be solved, one for each part. Note that the rigid transformation with parameters $\boldsymbol{\theta}$ added in the energy function (Eq. 3) helps to align the point sets. For instance, for the drill category shown in Figure 1, three shape spaces are required: base, top part, and shank.

The *hol+part* variant of our method is composed of two steps. In the first step, an initial registration takes place that registers the full geometry of the object in a holistic manner, i.e., the registration of the canonical model towards the observed one without any part decomposition. In the second step, a partwise
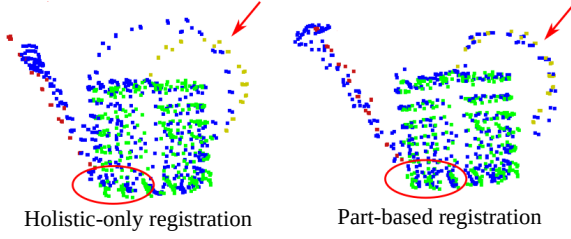
---

[1] http://ceres-solver.org

Figure 2: Holistic and partwise registration of a watering can with three parts: sprout (red), tank (green) and handle(gold). Note how the registration accuracy of the local structures (e.g., the handle) is improved by the part-based registration. The blue points represent the deforming point set.

registration is carried out, i.e., each individual part is registered. The holistic registration aims to capture global structures such as the dimensions of the object, while the objective of partwise registration is to improve registration accuracy of local structures.

The holistic registration serves as an initialization of the optimization for each of the parts. In this manner, Eq.(3) finds an optimum latent vector $\mathbf{x}_h$ and the parameters of a local registration $\boldsymbol{\theta}_h$. The values of $\boldsymbol{\theta}_h$ are passed directly to the optimization of each of the parts. However, the latent vector $\mathbf{x}_h$ cannot be passed directly, since each shape space represents the deformation fields of different shapes. The latent vector $\mathbf{x}_h$ maps to a deformation field $\mathbf{W}_h$. This matrix is separated in multiple matrices according to the part each deformation vector belongs to. By doing this, we avoid to perform an additional optimization that finds the latent vector of each part that matches the results of the holistic registration. On the other hand, this matrix separation assumes the contribution of deformation vectors of different parts as negligible. Because the holistic registration serves as initialization, the final result is given by the deformation vectors defined by each of the individual parts.

Both variants, i.e., the *partwise* and the *hol+part*, are evaluated in Section 4. Figure 2 shows the results of the non-rigid registration performed in a holistic-only and in a part-based manner. Note especially for the handle how the registration by parts improve the registration accuracy.

Our approach works directly on point sets but it can also be used to register meshes. An additional affinity matrix $\mathbf{G}(\mathbf{T}^m, \mathbf{T})$ is introduced for this purpose. This matrix maps the deformations from a point set $\mathbf{T}$ to the corresponding mesh vertices $\mathbf{T}^m$. The point set $\mathbf{T}$ of a mesh $\mathbf{T}^m$ is defined by ray-casting operations and a voxel filter. This results in a point cloud of uniform density. The deformed mesh vertices $\mathbf{C}^{m\prime}$ of the canonical mesh will be then defined
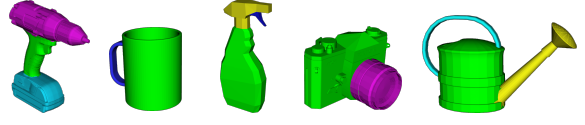

Figure 3: Canonical models of the evaluated categories: *drill*, *mug*, *spray bottle*, *camera* and *watering can* with the corresponding part decomposition.

as:

$$\mathbf{C}^{\mathbf{m}\prime} = \mathbf{C}^m + \mathbf{G}(\mathbf{C}^m, \mathbf{C}) * \mathbf{W}_i. \qquad (4)$$

4 EVALUATION

We tested the category-level part-based registration approach on five different categories: *drill* (17), *camera* (13), *spray bottle* (19), *watering can* (9), and *mug* (24). The number of instances for training the shape spaces are given inside parenthesis. Figure 3 presents the canonical model of each category with their part decomposition. The meshes were collected from online databases: Sketchfab[2], GrabCad[3], 3DWarehouse[4], and from the object meshes recently released in (Wang et al., 2019). For constructing the shape spaces, CPD is parametrized with $\lambda = 2$, $\beta = 2$ and 5 latent dimensions.

Our approach is evaluated with fully and partially observed shapes. All the testing instances are presented for the first time to our registration method. The partial views are generated by ray-casting a single view of the object from 42 different observation poses on a tessellated sphere, emulating what a robot
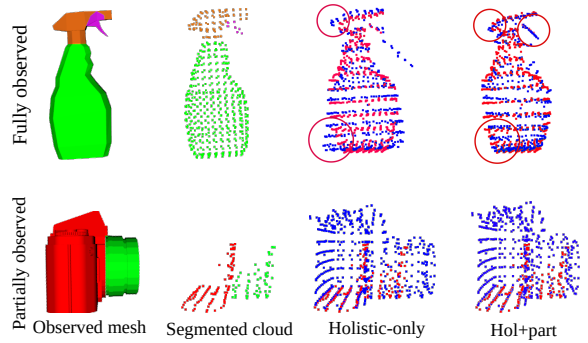

Figure 4: Results of the non-rigid registration performed on the *spraybottle* and *camera* categories by the *hol+part* variant of our approach, compared with a holistic registration. Observe how the quality of the local structures is improved by the part-based registration. The canonical deforming model is shown in blue. For clarity of the registered images, the observed instances are colored red.

---

[2] https://sketchfab.com/
[3] https://grabcad.com/library
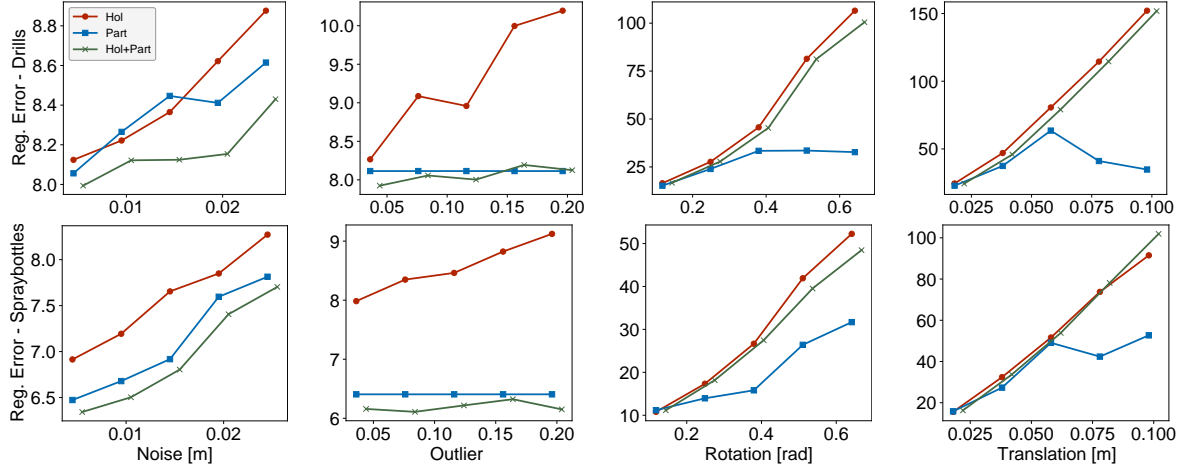[4] https://3dwarehouse.sketchup.com/

Figure 5: Average registration errors on full views of the *drill* and *spray bottle* categories with respect to different levels of noise, outliers, rotation and translation.

perceives in a real application. We compare the *partwise* and the *hol+part* variants of our method against the *holistic* registration that do not consider decomposed parts. Qualitative results of fully and partially observed instances are presented in Figure 4. Note how local structures are better captured by the registration on the part level.

In order to perform a quantitative evaluation, we define the following registration error:

$$E(\mathbf{T}, \mathbf{C}) = \frac{1}{M} \sum_{m=0}^{M-1} \min_{n} \|\mathbf{T}_n - \mathbf{C}_m\|^2, \qquad (5)$$

which aggregates a normalized distance to the closest point from the ground truth points $\mathbf{T}$. The numerical comparison between *partwise*, *hol+part* and *holistic* on complete ground truth observed instances is presented in Table 1. Observe that the *hol+part* variant outperforms the holistic-only and the partwise registration variant for fully observed models for all categories. This means that the registration by parts improves the overall accuracy and that an initial global registration is beneficial for initializing the subsequent partwise one with fully observed instances.

A similar evaluation is performed on partially observed instances whose results are presented in Ta-

Table 1: Average registration error on the evaluated categories with fully observed instances.

	Holistic	Partwise	Hol+Part
Camera	3.96	3.96	**3.67**
Drill	7.19	7.06	**7.04**
Mug	5.21	5.41	**5.20**
Spray bottle	7.60	7.22	**7.05**
Watering can	18.72	15.61	**15.55**

Table 2: Average registration error on the evaluated categories with 42 partial views.

	Holistic	Partwise	Hol+Part
Camera	0.241	**0.20**	0.24
Drill	0.67	**0.64**	0.68
Mug	**0.21**	0.22	0.22
Spray bottle	**0.64**	0.65	0.68
Watering can	1.99	**1.84**	1.90

ble 2. Note that when objects are not complete, the *hol+part* variant does not perform well compared to the other two methods. With partial views, some parts might have very few points and their contribution to the holistic registration is low, for this reason, using the result of an initial holistic registration might lead to a bad initialization for the subsequent partwise registration.

We also evaluate the robustness of our approach against different degrees of noise, outliers, rotation and translation. We initially add noise to the position of the observed point set. This noise is sampled from a Gaussian distribution with zero mean. The value of the standard deviation is increased gradually from 0.005 to 0.025. Secondly, outliers are incorporated to the observed instances, i.e., the position of the observed points is not altered but random points sampled from a Uniform distribution inside the bounding box of the object are added. The ratio of number of outliers goes from 0.04 to 0.2. We also analyze the effect of having errors on the observed object pose. We consider rotation and translation separately. We rotate the observed instance in each of the global *x*-, *y*- and *z*-axis consecutively with the same angle. The direction of rotation of each axis is randomized. The angle values goes from 0.13 to 0.65 rad with a step of
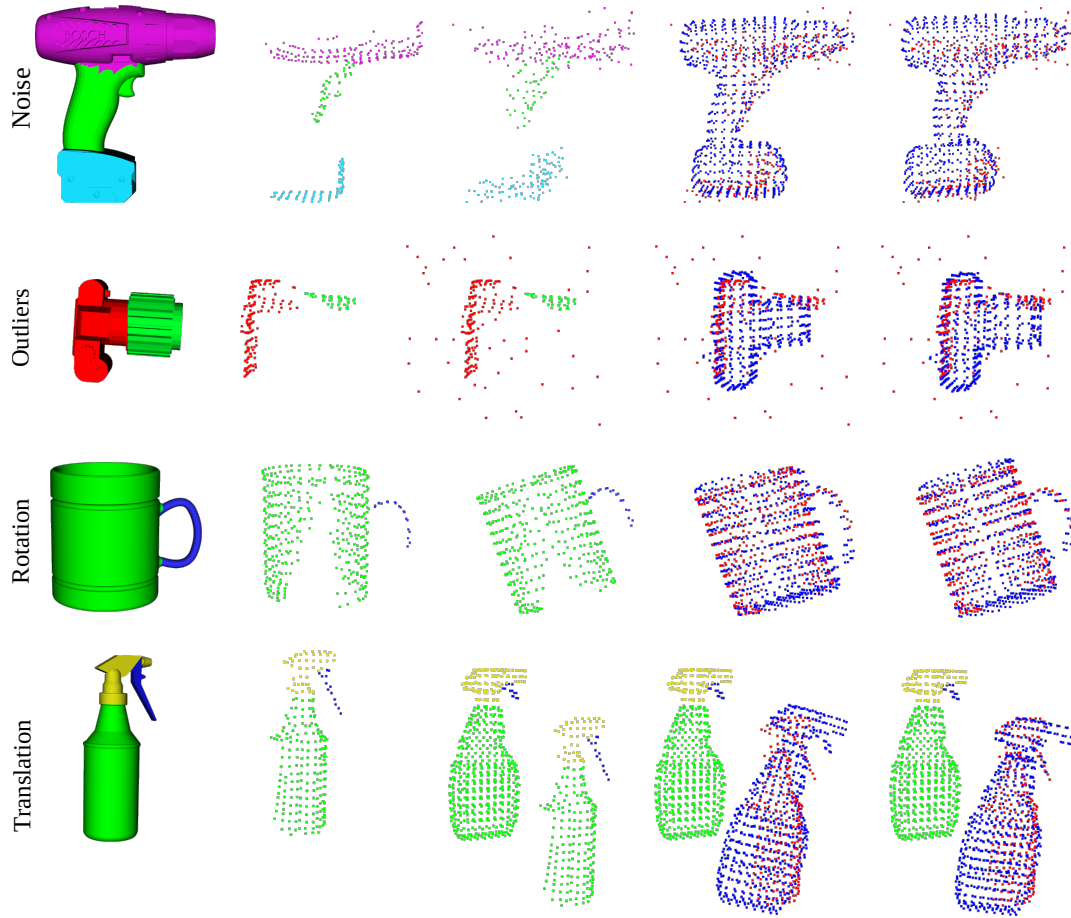
Figure 6: Registration results of the holistic-only and part-based registration on partial views on four different categories with noise, outliers, rotation and translation. The aim is to deform the canonical model (blue) onto the observed instances (red). The first three columns show the observed models with the segmented parts. For clarity in the registered images, the observed instances are completely colored red. Observe how the registration accuracy of the lens of the camera, the handle of the mug and the trigger of the spray bottle is improved by the part-based registration. For the translation, the canonical model is also presented to indicate the observed object pose.
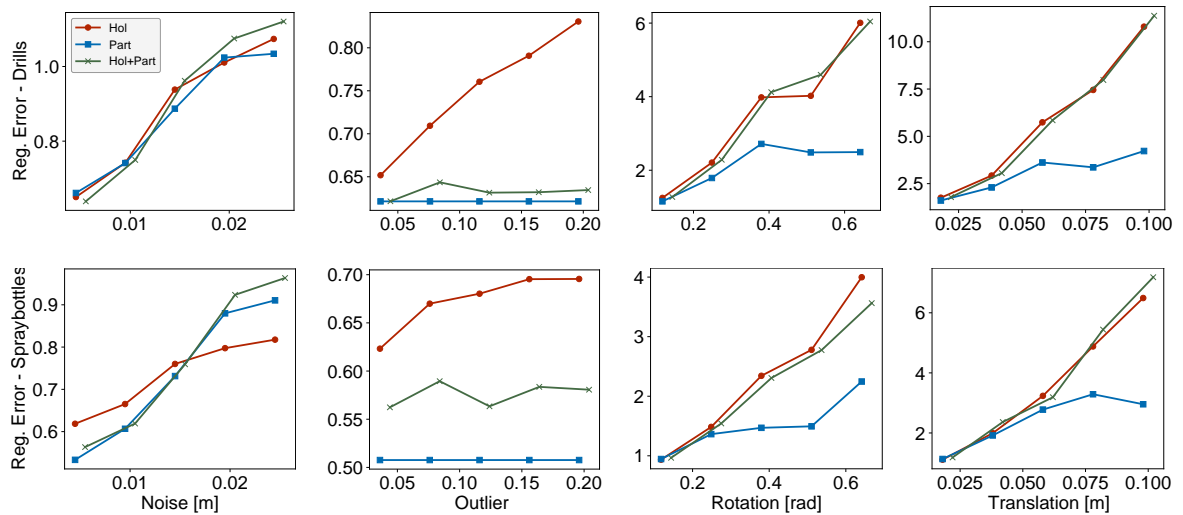

Figure 7: Average registration errors on partial views of the *drill* and *spray bottle* categories with respect to different levels of noise, outliers, rotation and translation. Each point represents the mean error over 42 partial views.

0.13 rad. Finally, the observed instance is translated in all three axes from 0.02 to 0.1 m. Examples of the altered observed instances with the noise, outliers, rotation and translation together with their corresponding *holistic* and *hol+part* registrations are presented in Figure 6. Note how local geometries such as the lens of the camera, the handle of the mug and the trigger of the spray bottles are better captured with the *hol+part* registration.

Numerical results of the drill and spray bottle categories with fully observed instances are presented in Figure 5. Figure 7 reports the average registration errors of partial views. Only two categories are presented but the remaining three behave similarly. The *hol+part* variant continues outperforming the other two methods with noise and outliers on fully observed instances. However, for rotation and translation, the *partwise* variant is more robust, which implies that misalignments on a global level of the object are more difficult to refine. Moreover, on partial views the *partwise* variant continues outperforming the other two methods and is more robust against noise, outliers rotation and translation.

5 CONCLUSION

In this paper, we have presented a novel part-based non-rigid registration method that improves the accuracy of local structures by registering individually decomposed parts of the object. The method is based on learned shape spaces of each of the decomposed parts. We have shown in the experimental section that a holistic registration followed by a partwise registration (*hol+part*) is very effective for registering fully observed objects, while a partwise registration performs better with partial views. We demonstrated the robustness of our approach against noise, outliers and misalignments in rotation and translation. In the future, we plan to investigate hierarchies and dependencies between parts of more complex objects. Moreover, we will evaluate the strengths and limitations of the part-based registration when applied to grasping skill transfer methods.

REFERENCES

Adeshina, S. A. and Cootes, T. F. (2010). Evaluation of performance of part-based models for groupwise registration. *Medical Image Understanding and Analysis Conf. (MIUA)*, pages 221–251.

Aleotti, J. and Caselli, S. (2011). Part-based robot grasp planning from human demonstration. In *IEEE Int. Conf. on Robotics and Automation (ICRA)*, pages 4554–4560.

Aleotti, J., Rizzini, D. L., and Caselli, S. (2014). Perception and grasping of object parts from active robot exploration. *Journal of Intelligent & Robotic Systems (JINT)*, 76(3):401–425.

Allen, B., Curless, B., and Popović, Z. (2003). The space of human body shapes: Reconstruction and parameterization from range scans. *ACM Transactions on Graphics (TOG)*.

Araslanov, N., Koo, S., Gall, J., and Behnke, S. (2016). Efficient single-view 3D co-segmentation using shape similarity and spatial part relations. In *German Conf. on Pattern Recognition (GCPR)*, pages 297–308.

Blanz, V. and Vetter, T. (1999). A morphable model for the synthesis of 3D faces. In *Proc. of the 26th Conf. on Computer Graphics and Interactive Techniques (SIGGRAPH)*, pages 187–194.

Burghard, O., Berner, A., Wand, M., Mitra, N., Seidel, H.-P., and Klein, R. (2013). Compact part-based shape spaces for dense correspondences. *arXiv preprint arXiv:1311.7535*.

Chui, H. and Rangarajan, A. (2003). A new point matching algorithm for non-rigid registration. *Computer Vision and Image Understanding (CVIU)*, pages 114–141.

Engelmann, F., Stückler, J., and Leibe, B. (2016). Joint object pose estimation and shape reconstruction in urban street scenes using 3D shape priors. In *German Conf. on Pattern Recognition (GCPR)*.

Haehnel, D., Thrun, S., and Burgard, W. (2003). An extension of the ICP algorithm for modeling nonrigid objects with mobile robots. In *Int. Joint Conf. on Artificial Intelligence (IJCAI)*.

Hasler, N., Stoll, C., Sunkel, M., Rosenhahn, B., and Seidel, H.-P. (2009). A statistical model of human pose and body shape. In *Computer Graphics Forum (Eurographics)*.

Horaud, R., Forbes, F., Yguel, M., Dewaele, G., and Zhang, J. (2010). Rigid and articulated point registration with expectation conditional maximization. *IEEE Transactions on Pattern Analysis and Machine Intelligence (TPAMI)*, pages 587–602.

Huang, Q.-X., Zhang, G.-X., Gao, L., Hu, S.-M., Butscher, A., and Guibas, L. (2012). An optimization approach for extracting and encoding consistent maps in a shape collection. *ACM Transactions on Graphics (TOG)*, page 167.

Kim, V. G., Lipman, Y., and Funkhouser, T. (2011). Blended intrinsic maps. In *ACM Transactions on Graphics (TOG)*.

Krebs, J., Mansi, T., Delingette, H., Zhang, L., Ghesu, F. C., Miao, S., Maier, A. K., Ayache, N., Liao, R., and Kamen, A. (2017). Robust non-rigid registration through agent-based action learning. In *Int. Conf. on Medical Image Computing and Computer-Assisted Intervention (MICCAI)*, pages 344–352.

Ma, J., Zhao, J., and Yuille, A. L. (2016). Non-rigid point set registration by preserving global and structures. *IEEE Transactions on Image Processing*, pages 53–64.

Marsland, S., Twining, C. J., and Taylor, C. J. (2003). Groupwise non-rigid registration using polyharmonic clamped-plate splines. In *Int. Conf. on Medical Image Computing and Computer-Assisted Intervention (MICCAI)*, pages 771–779.

Myronenko, A. and Song, X. (2010). Point set registration: Coherent point drift. *IEEE Transactions on Pattern Analysis and Machine Intelligence (TPAMI)*.

Nguyen, A., Ben-Chen, M., Welnicka, K., Ye, Y., and Guibas, L. (2011). An optimization approach to improving collections of shape maps. In *Computer Graphics Forum*, pages 1481–1491.

Ovsjanikov, M., Mérigot, Q., Mémoli, F., and Guibas, L. (2010). One point isometric matching with the heat kernel. In *Computer Graphics Forum*.

Palafox, P., Božič, A., Thies, J., Nießner, M., and Dai, A. (2021). NPMs: Neural parametric models for 3D deformable shapes. *arXiv:2104.00702*.

Rodriguez, D. and Behnke, S. (2018). Transferring category-based functional grasping skills by latent space non-rigid registration. In *IEEE Robotics and Automation Letters (RA-L)*, volume 3, pages 2662–2669.

Rodriguez, D., Cogswell, C., Koo, S., and Behnke, S. (2018). Transferring grasping skills to novel instances by latent space non-rigid registration. In *IEEE International Conference on Robotics and Automation (ICRA)*.

Stouraitis, T., Hillenbrand, U., and Roa, M. A. (2015). Functional power grasps transferred through warping and replanning. In *IEEE Int. Conf. on Robotics and Automation (ICRA)*.

Stueckler, J., Steffens, R., Holz, D., and Behnke, S. (2011). Real-time 3D perception and efficient grasp planning for everyday manipulation tasks. In *European Conf. on Mobile Robots (ECMR)*, pages 177–182.

Tevs, A., Bokeloh, M., Wand, M., Schilling, A., and Seidel, H.-P. (2009). Isometric registration of ambiguous and partial data. In *IEEE Conf. on Computer Vision and Pattern Recognition (CVPR)*.

Vahrenkamp, N., Westkamp, L., Yamanobe, N., Aksoy, E. E., and Asfour, T. (2016). Part-based grasp planning for familiar objects. In *IEEE-RAS 16th Int. Conf. on Humanoid Robots (Humanoids)*, pages 919–925.

Wang, H., Sridhar, S., Huang, J., Valentin, J., Song, S., and Guibas, L. J. (2019). Normalized object coordinate space for category-level 6D object pose and size estimation. In *The IEEE Conf. on Computer Vision and Pattern Recognition (CVPR)*.

Xiong, L., Wu, L., Cui, W., Zhang, S., Xu, G., and Hu, H. (2018). Robust non-rigid registration based on affine ICP algorithm and part-based method. *Neural Processing Letters*, 48(3):1305–1321.

Zeng, Y., Wang, C., Wang, Y., Gu, X., Samaras, D., and Paragios, N. (2010). Dense non-rigid surface registration using high-order graph matching. In *IEEE Conf. on Computer Vision and Pattern Recognition (CVPR)*.

Zollhöfer, M., Nießner, M., Izadi, S., Rehmann, C., Zach, C., Fisher, M., Wu, C., Fitzgibbon, A., Loop, C.,

Theobalt, C., et al. (2014). Real-time non-rigid reconstruction using an RGB-D camera. *ACM Transactions on Graphics (TOG)*, page 156.

Zou, G., Hua, J., and Muzik, O. (2007). Non-rigid surface registration using spherical thin-plate splines. In *Int. Conf. on Medical Image Computing and Computer-Assisted Intervention (MICCAI)*, pages 367–374.